

REPORT DOCUMENTATION FORM
WATER RESOURCES RESEARCH CENTER
University of Hawaii at Manoa

¹ Report Number Technical Memorandum Report No. 66	² FCST Category 04-B
³ Title <i>Formation of Transition Zone in a Basal Aquifer Under Pumping Stresses</i>	⁴ Report Date August 1982
	⁵ No. of Pages viii + 21 p.
	⁶ No. of Tables 2
⁸ Author(s) Mr. Sang-Ok Chung Dr. L. Stephen Lau Dr. Clark C.K. Liu Mr. Henry K. Gee	⁹ Grant Agency Office of Water Policy, U.S. Department of the Interior
	¹⁰ Grant/Contract No. 14-34-0001-2113 (A-092-HI)
¹¹ Descriptors: *Aquifer characteristics, *Transition zones, *Saline water-freshwater interfaces, Experimental data, Hawaii Identifiers: *Sand-box model	
¹² Abstract (Purpose, method, results, conclusions) Formation of a freshwater-sea water transition zone in a basal aquifer under pumping stresses was studied by sand-box experiments and by comparing experimental data with results from other theoretical and field investigations. Upconing height for different pumping rates and well penetration depths were measured in the laboratory. These experimental data were then compared with theoretical values computed with or without the sharp interface assumption. Dispersivity of laboratory sand was determined by matching the observed thickness of the transition zone with the theoretical value. The thickness of the transition zone was found to increase as the pumping rate and/or the partial well penetration depth increased. The results of the laboratory experiments were compatible with the values predicted by theoretical equations.	

FORMATION OF TRANSITION ZONE IN A
BASAL AQUIFER UNDER PUMPING STRESSES

Sang-Ok Chung

L. Stephen Lau

Clark C.K. Liu

Henry K. Gee

Technical Memorandum Report No. 66

August 1982

Research Project Technical Completion Report
for
Evolution of Freshwater-Saltwater Transition Zone
in a Coastal Aquifer under Pumping Stress
Project A-092-HI

Grant Agreement No.: 14-34-0001-2113

Project Investigator: L. Stephen Lau

Prepared for
UNITED STATES DEPARTMENT OF THE INTERIOR

The work upon which this report is based was supported in part by federal funds provided by the United States Department of the Interior, as authorized under the Water Research and Development Act of 1978, as amended.

WATER RESOURCES RESEARCH CENTER
University of Hawaii at Manoa
Honolulu, Hawaii 96822

AUTHORS:

Mr. Sang-Ok Chung
Former Graduate student
Water Resources Research Center
University of Hawaii at Manoa

Dr. L. Stephen Lau
Director, Water Resources Research Center
Professor, Department of Civil Engineering
University of Hawaii at Manoa

Dr. Clark C.K. Liu
Assistant Professor
Department of Civil Engineering
University of Hawaii at Manoa

Mr. Henry K. Gee
Research Associate
Water Resources Research Center
University of Hawaii at Manoa

Contents of this publication do not necessarily reflect the views and policies of the United States Department of the Interior, nor does mention of trade names or commercial products constitute their endorsement or recommendation for use by the United States Government

\$2.00/copy

Checks payable to: Research Corporation, University of Hawaii

Mail to: University of Hawaii at Manoa
Water Resources Research Center
2540 Dole St., Holmes Hall 283
Honolulu, Hawaii 96822

Tel.: (808) 948-7847 or -7848

ABSTRACT

Formation of a freshwater-sea water transition zone in a basal aquifer under pumping stresses was studied by sand-box experiments and by comparing experimental data with results from other theoretical and field investigations.

Upconing height for different pumping rates and well penetration depths were measured in the laboratory. These experimental data were then compared with theoretical values computed with or without the sharp interface assumption. Dispersivity of laboratory sand was determined by matching the observed thickness of the transition zone with the theoretical value.

The thickness of the transition zone was found to increase as the pumping rate and/or the partial well penetration depth increased. The results of the laboratory experiments were compatible with the values predicted by theoretical equations.

CONTENTS

	Page
ABSTRACT.	v
INTRODUCTION.	1
OBJECTIVES.	1
EXPERIMENTAL SETUP.	1
EXPERIMENTAL PROCEDURES	4
EXPERIMENTAL RESULTS.	10
DATA INTERPRETATION AND DISCUSSIONS	10
Upconing with Sharp Interface.	10
Determination of Dispersivity of Laboratory Sand	16
Upconing with Transition Zone.	19
CONCLUSIONS AND RECOMMENDATIONS	20
REFERENCES.	20

Figures

1. Experimental Setup of Sand Box, Well, and Sea Water Reservoir.	2
2. Sand Box Schematic	3
3. Relation Between Initial Interface (50% Relative Concentration) and Interface Based on Ghyben-Herzberg Relationship.	5
4. Movement Pattern of Fluorescein and Rhodamine B at a Well Penetration of 27.31 in. and at a Pumping Rate of 180 ml/min	6
5. Movement Pattern of Fluorescein and Rhodamine B at a Well Penetration of 29.56 in. and at a Pumping Rate of 180 ml/min	7
6. Movement Pattern of Sea Water at a Well Penetration of 33.75 in. and at a Pumping Rate of 80 ml/min.	7
7. Movement Pattern of Injected Dye Solution at Equilibrium Condition at 5 min after Injection	8
8. Movement Pattern of Injected Dye Solution at Equilibrium Condition at 30 min after Injection.	8
9. Upconing Height vs. Elapsed Pumping Time	13

10. Effect of Well Penetration and Pumping Rate on Upconing Height.	13
11. Dimensionless Upconing Height vs. Dimensionless Partial Well Penetration	14
12. Dispersivity for Different Pumping Rates	18

Tables

1. Salinity, Conductivity, and Relative Concentration of Selected Samples	11
2. Upconing Height and Thickness of Transition Zone Directly Beneath Well	15

INTRODUCTION

Upconing of sea water in a basal aquifer is one of the most important groundwater management issues in determining pumping rate and duration, and the penetration depth of wells.

When the freshwater overlying the saline water is pumped by a well, the saline water may move upward. This phenomenon is commonly called upconing. For the case of immiscible liquids, the factors controlling upconing presented by Bear and Dagan (1964) included: pumping rate, depth below the well bottom to the interface, lateral distance from the well, duration of pumping, horizontal permeability of the aquifer, density difference between the fresh and saline waters, and porosity of the aquifer.

Hydrodynamic dispersion also influences the upconing height. A transition zone between fresh and saline waters always exists as a result of hydrodynamic dispersion. Hydrodynamic dispersion, which is a combination of mechanical dispersion, molecular diffusion, and interface mass transfer, widens the initially sharp interface between fresh and saline waters (Schmorak and Mercado 1969).

OBJECTIVES

A laboratory sand-box model was used to study an approximated one-dimensional saline water-freshwater interface movement and hydrodynamic dispersion phenomena. The experiments are intended to be preliminary but sufficiently qualitative to provide insight. However, precision was not the principal objective. The experiments were controlled to produce an approximately horizontal interface with an approximately vertical flow pattern. Those experiments that produced pronounced curvature of the interface by two rather than the approximately one-dimensional flow were not included in the analysis although they were run. However, the rising phenomenon is herein referred to as upconing using conventional terminology.

EXPERIMENTAL SETUP

The experimental system consisted of a sand box, a well, and a sea water reservoir (Fig. 1). The sand box was constructed of 4.76 mm (3/16 in.)

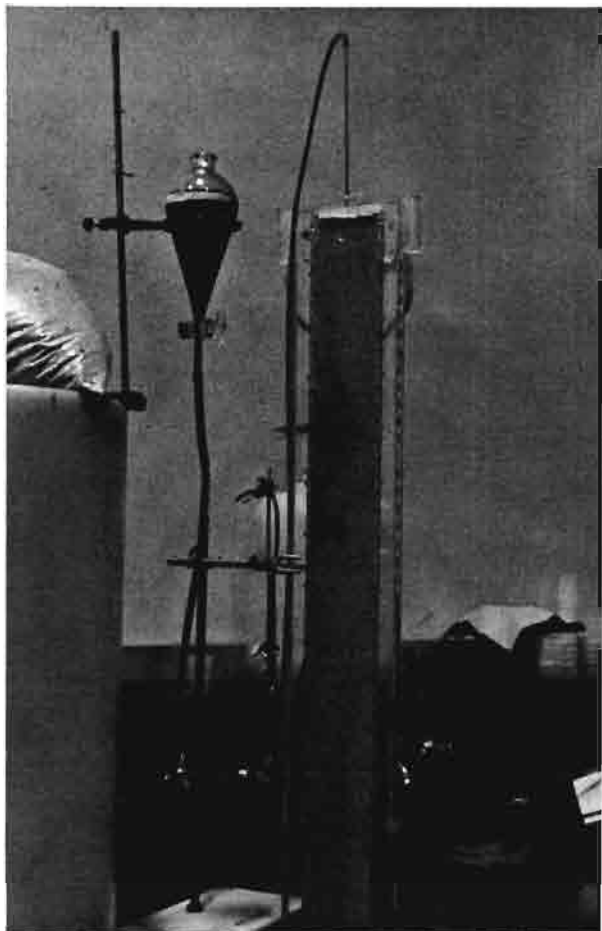


Figure 1. Experimental setup of sand box, well, and sea water reservoir

thick Plexiglas and consisted of one center and two side compartments. Fresh water flowed from the side chambers into the center chamber through holes drilled in the walls that separated the chambers. Each side compartment had an overflow weir. The inside dimensions of the sand box were 1.052 m (41-13/32 in.) high by 0.013 m ($\frac{1}{2}$ in.) thick, and by 0.102 m (4 in.) and 0.025 m (1 in.) widths for the respective center and side compartments (Fig. 2). To equalize the piezometric heads, the two side chambers were interconnected by rubber tubing attached to 0.013 m Plexiglas inserts. Side chambers supplied water to replace water drawn out by the well. Rubber septums, which were used for extracting samples and injecting dyes with a hypodermic syringe, were installed on one side of the center chamber.

A 500 ml separatory funnel used as a sea water reservoir was connected to the bottom of the center chamber with a rubber tube. The well was a

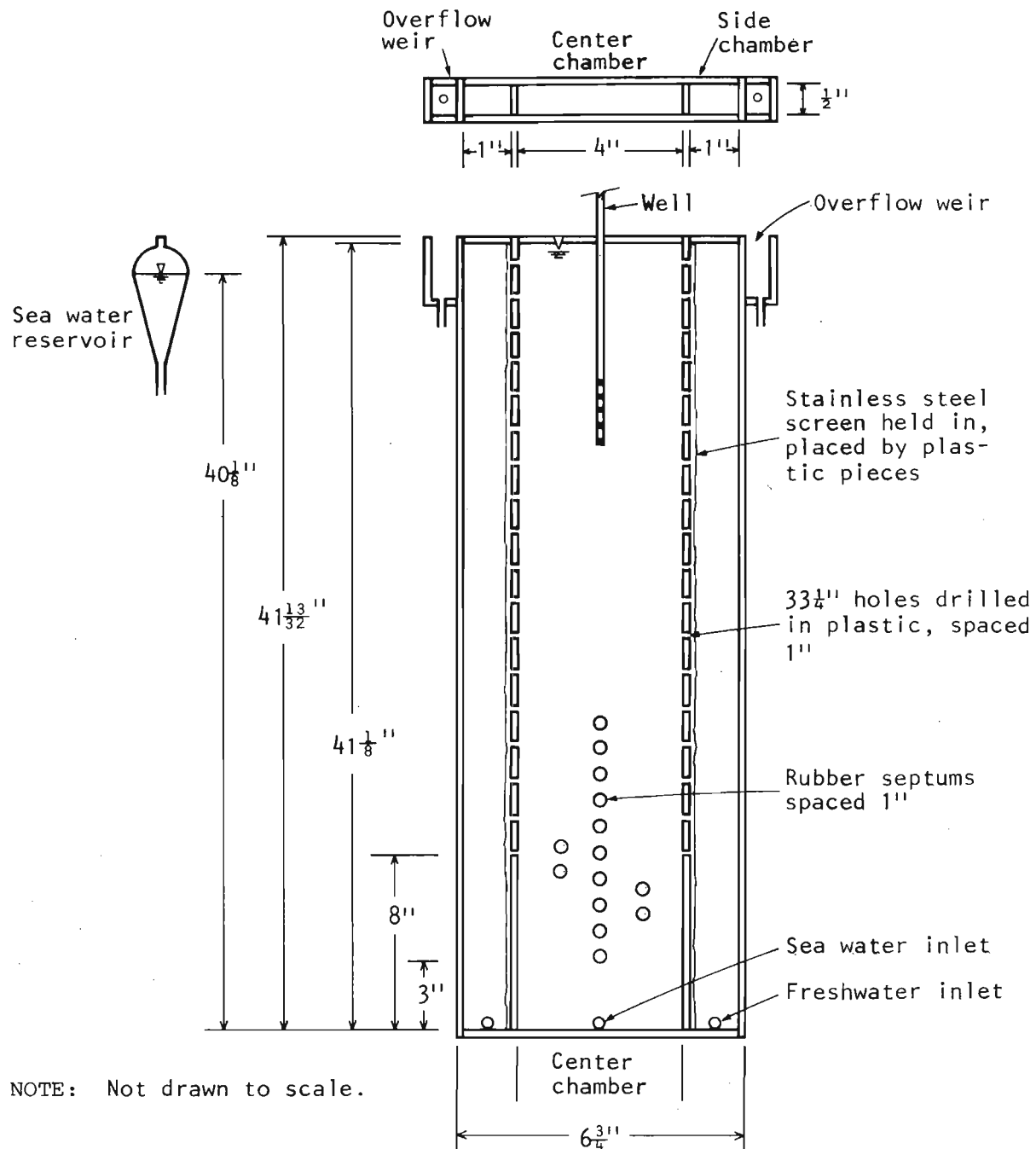


Figure 2. Sand-box schematic

brass tube with a 2.38 (3/32 in.) outer diameter that had been drilled with a No. 6 drill bit (1.016-mm [0.04-in.] diam). The holes were spaced at 1.59-mm (1/16-in.) intervals and aligned 120° apart. The total length of the perforation was 0.06 m (2-3/8 in.) and the total length of the brass well was 0.97 m (38 in.). The wall was connected with a rubber tube which siphoned out water.

EXPERIMENTAL PROCEDURES

To prevent the formation of air bubbles in the sand aquifer, the center chamber was first filled with water and sand was then funneled into the chamber through the top opening. The sand was screened through a No. 16 sieve and settled onto a No. 30 sieve in which the sand was packed by striking the outside of the chamber with a rubber hammer. When the height of the sand was raised slightly above the predetermined well bottom position, the well was placed in the model and the chamber was filled with sand in the same way to just slightly below the height of the overflow weirs.

Sea water taken offshore of Magic Island on O'ahu was mixed with rhodamine B and fluorescein dyes so that its movement could be traced by visual observation. Since fluorescein disperses more than rhodamine B does, the two dyes registered two different visual interfaces. The concentration of rhodamine B and fluorescein were respectively 0.4 and 1.5 g/l. The density of dyed sea water was not measured but might approximate 1.025. The sea water level was adjusted to raise the freshwater level in the center chamber about 0.025 m above the sea water level. The depth to the sea water-freshwater interface below the sea water level would then be 1.016 m (40 in.) according to the Ghyben-Herzberg relation. The heights of the sea water and freshwater levels are shown in Figure 3.

Fresh water was supplied from tap water at a rate to provide a slight overflow through the weirs at all times. Sea water dyed with a mixture of rhodamine B and fluorescein was introduced into the center chamber at the bottom and allowed to reach an equilibrium condition after 10 to 16 hr periods.

At the equilibrium condition, the sea water level and freshwater level were marked with tape on the separatory funnel and on the sand box, respectively. A siphon was then used to start pumping fresh water from the well. By changing the height of the outlet of the rubber tube siphon connected to the well, the pumping rates were controlled.

A total of four runs were made in this study. Four different well penetration depths from the freshwater table in their order of utilization were 0.55, 0.69, 0.75, and 0.86 m (21.72, 27.31, 29.56, and 33.75 in.). Each run, except the last run with a 0.86 m well penetration depth, was conducted for three different predetermined pumping rates of 80, 130, and

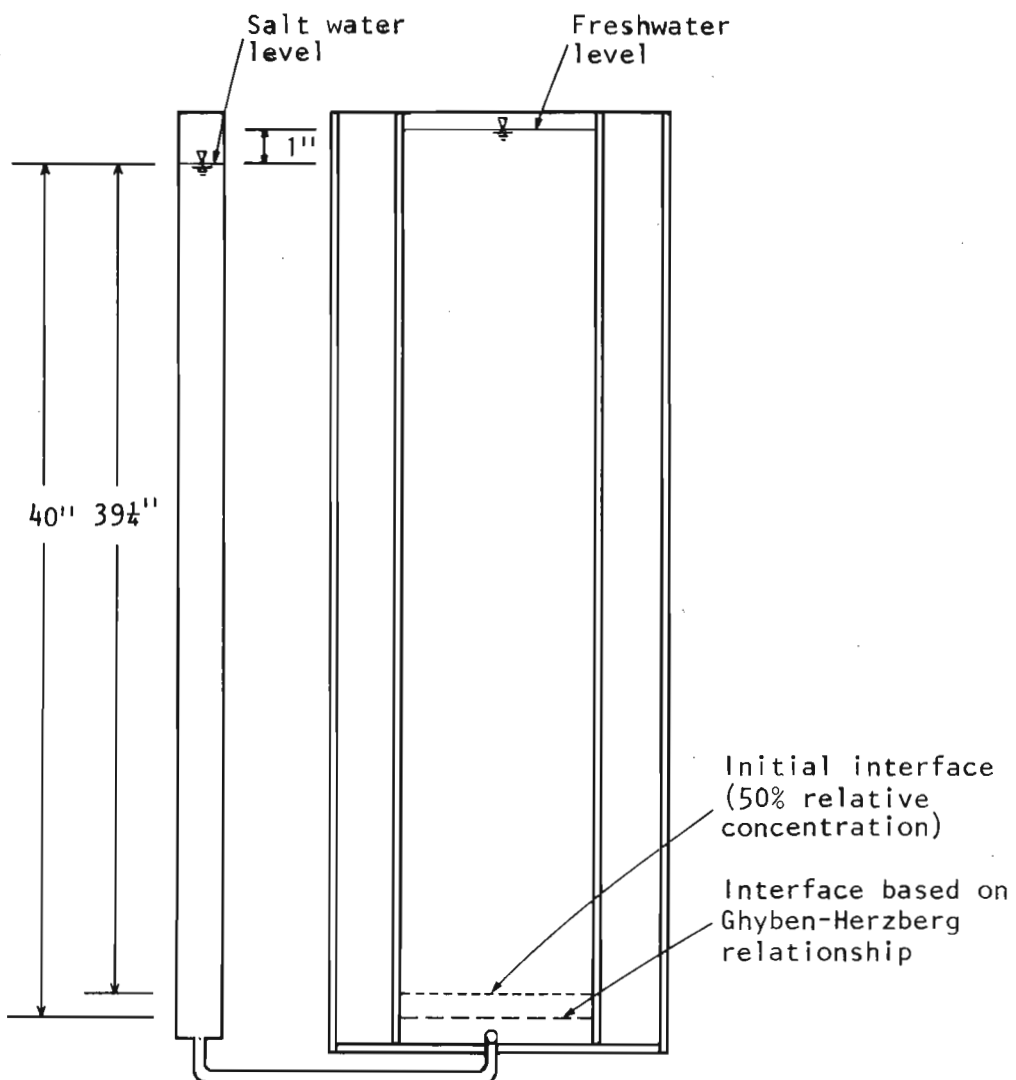


Figure 3. Relation between initial interface (50% relative concentration) and interface based on Ghyben-Herzberg relationship

180 ml/min. For the 0.86 m well penetration, the dyed sea water reached the well at the 80 ml/min pumping rate; therefore no greater pumping rate was tried.

At the beginning of each run, the lowest (80 ml/min) pumping rate was applied. To maintain a constant freshwater level as marked previously, the tap water supply was appropriately increased. As the fresh water was pumped, the sea water-freshwater interface moved upward. Consequently, the sea water level in the reservoir was lowered. To maintain a constant sea water level as marked previously, the dyed sea water was added continuously into the reservoir by using a pipet. During the pumping, the sea water-freshwater

interface was marked and the upconing height was measure for the upper boundary of fluorescein zone and the fluorescein-rhodamine B interface, as illuminated by an ultraviolet light source, at several time intervals. The pumping was continued until a new equilibrium condition was reached. The pumping was then increased to 130 ml/min by lowering the outlet of the siphon tube. The same procedures were followed and the pumping rate was then increased to 180 ml/min, following the same procedures.

Figures 4, 5, and 6 show movement patterns of fluorescein and rhodamine B with respect to pumping rate.

At the equilibrium condition of the third run with a pumping rate of 180 ml/min (Fig. 7), a dye solution of fresh water with 0.4 g/l concentra-

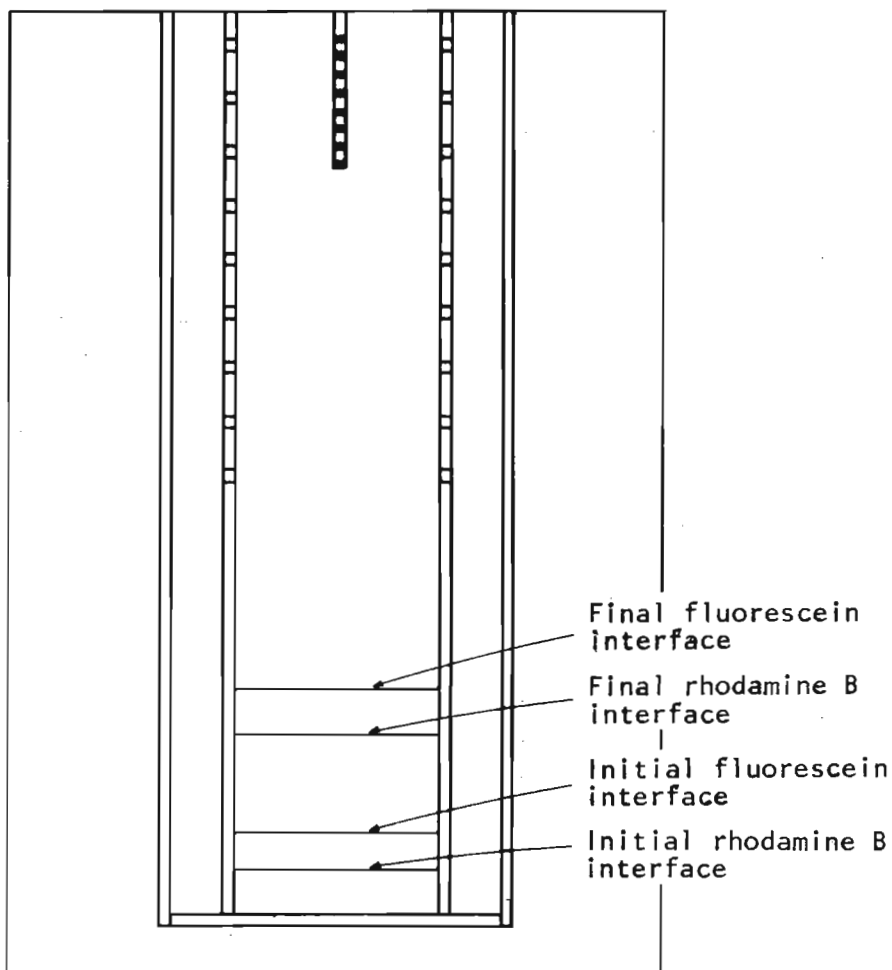


Figure 4. Movement pattern of fluorescein and rhodamine B at a well penetration of 27.31 in. and at a pumping rate of 180 ml/min

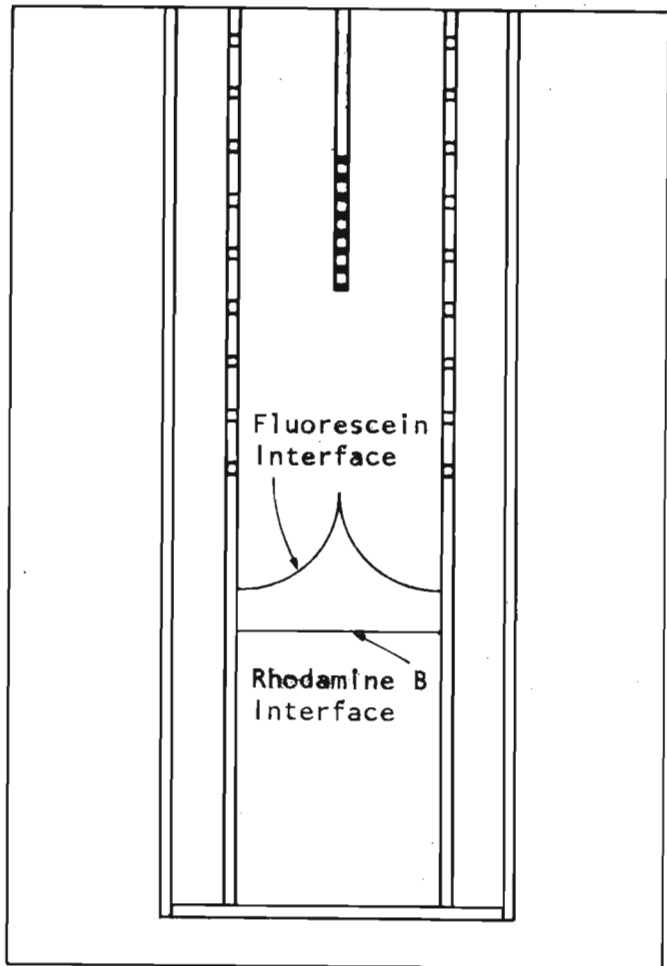
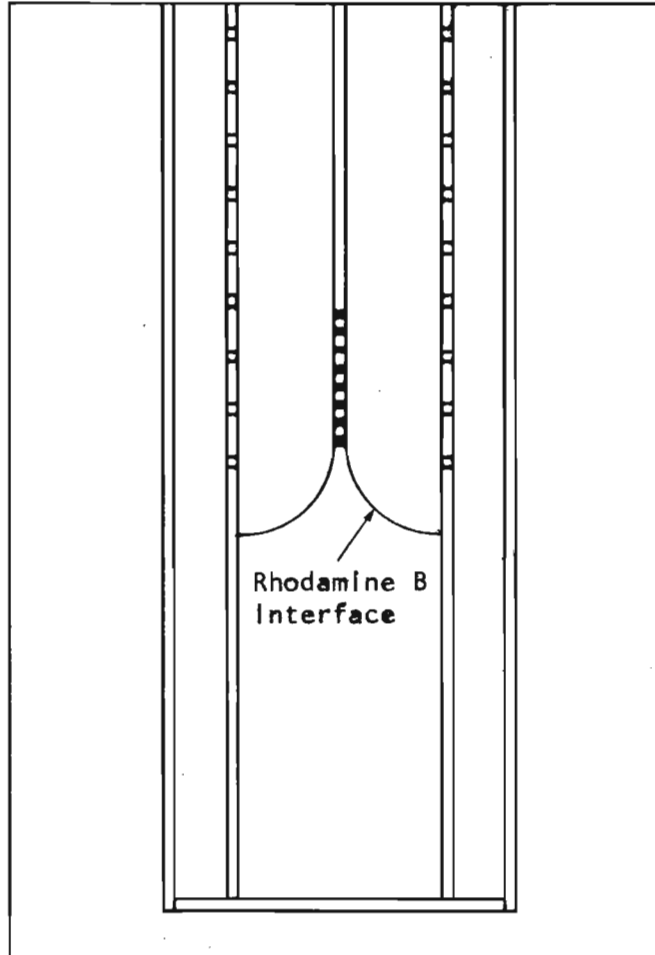
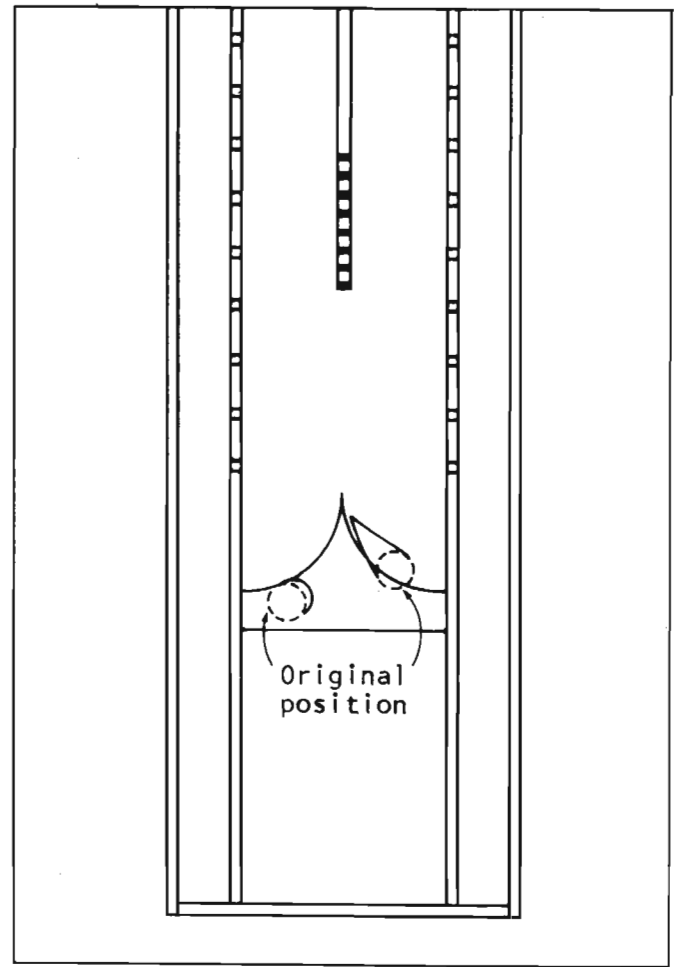


Figure 5. Movement pattern of fluorescein and rhodamine B at a well penetration of 29.56 in. and at a pumping rate of 180 ml/min



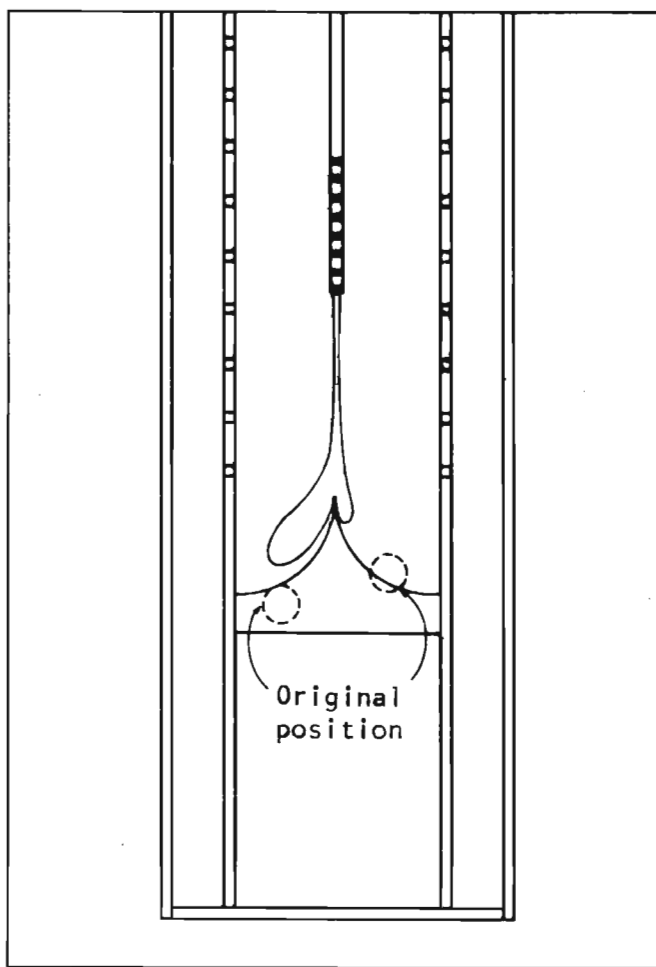
NOTE: Two hours after onset of pumping, sea water reached the well. Fluorescein zone had already entered well and was no longer observed.

Figure 6. Movement pattern of sea water at a well penetration of 33.75 in. and at a pumping rate of 80 ml/min



NOTE: Well depth 29.56 in., pumping rate
180 ml/min.

Figure 7. Movement pattern of injected dye solution at equilibrium condition at 5 min after injection



NOTE: Well depth 29.56 in., pumping rate
180 ml/min.

Figure 8. Movement pattern of injected dye solution at equilibrium condition at 30 min after injection

tion of rhodamine B was injected through septums on the inclined fluorescein interface and the dye movement were observed. Figures 7 and 8 show the dye movement at 5 and 30 min, respectively, after injection. At 30 min after the dye on the right-hand side reached the well and completely disappeared from the original position, the dye on the left-hand side, which was farther than the right-hand side dye from the well center axis, was still moving toward the well bottom. Although the dye reached the well, no sea water was observed in the pumped water from salinity and electrical conductivity measurements.

Salinity and electrical conductivity were measured for fresh water, sea water and for samples extracted with a hypodermic syringe using a salinity conductivity meter (YSI Model 33). The samples extracted had volumes of 5 to 20 mL and were diluted with distilled water to obtain volumes of 100 mL, the minimum volume required for the measurements.

After finishing all the observations of a run, the sand in the model was removed and replaced with new sand for the next run.

The porosity and vertical hydraulic conductivity of the sand aquifer were measured following the *ASTM Standards* (ASTM 1980). For the porosity measurement, the specific gravity of the sand was measured using a pycnometer, and the dry density was measured by the oven drying method. Then, the void ratio was computed using the specific gravity and the dry density. Porosity was then computed from the void ratio.

For the vertical hydraulic conductivity measurement, a simplified permeameter modified from the *ASTM Standards* was used. The permeameter consisted of a specimen cylinder and a lower water basin. The specimen cylinder, which had an overflow weir 0.10 m (4 in.) in diameter and 0.15 m (6 in.) in height, was filled up to 0.10 m with sand. The sand was packed in the same way as the sand box to obtain a porosity close to that of the sand box. The cylinder was placed on a platform inside the lower basin which had an overflow weir 0.30 m (12 in.) in diameter and 0.20 m (8 in.) in height. Tap water applied over the sand specimen flowed downward through the specimen into the lower basin. The water level in the sand specimen was maintained at a constant level. At the equilibrium condition, the overflow rate through the lower basin weir, head difference and discharge time were measured and the permeability was calculated.

EXPERIMENTAL RESULTS

Below the freshwater lens under an ultraviolet light source were two different colored zones: one was yellowish green on the top, the other was red, which represented respectively the fluorescein zone and the rhodamine B zone. The thickness of the fluorescein zone at the initial equilibrium condition, varied from 6.35 to 19.05 mm (0.25-0.75 in.). After pumping they varied from 8.64 to 24.64 mm (0.34-0.97 in.). This confirms the well known widening of the sea water-freshwater transition zones after pumping.

All the interfaces of the fluorescein zone and rhodamine B zone after pumping were horizontal except during the third run (0.75 m well penetration) with a 180 ml/min pumping rate and the fourth run (0.86 m well penetration) with an 80 ml/min pumping rate. The third and fourth runs had inclined interfaces and deeper well penetration depths than the first and second runs. Since those inclined interfaces cannot be represented by the one-dimensional upconing equation, they were excluded from the analyses. Table 1 shows measured salinity, electrical conductivity, and relative salinity of selected samples.

The porosity and vertical hydraulic conductivity, K_z , of the sand aquifer were respectively 38% and 0.002 m/s (481 ft/day).

DATA INTERPRETATION AND DISCUSSIONS

Upconing with Sharp Interface

In many previous upconing studies, a sharp interface between the fresh water and the underlying saline water was often assumed (Bear 1972; Chandler and McWhorter 1975; Todd 1974). This approach is considered to be acceptable in many practical applications, since the transition zone between the fresh water and salt water is often narrow relative to the size of the flow domain (Bear 1972, 1979). The assumption of an abrupt interface has the advantage of simplicity (Bear 1972; Todd 1974). In this experiment, although a transition zone was clearly developed, the sharp interface assumption was first employed in the data interpretation. Hydrodynamic dispersion and transition zone evolution will be introduced in the following sections.

As in most past studies (Todd 1974; Bear and Dagan 1964; Schmorak and Mercado 1969; Visher and Mink 1964), the "sharp" interface elevations be-

TABLE 1. SALINITY, CONDUCTIVITY, AND RELATIVE CONCENTRATION OF SELECTED SAMPLES

Sample	Salinity (%)	Conduc- tivity ($\mu\text{mhos}/\text{cm}$)	Relative Concentration (%)
Fresh water.....	0.3	340	0
Dyed sea water.....	29.0	44,000	100
Fluorescein upper boundary..... (27.3 in. well depth; 180 ml/min pumping rate)	6.5	11,150	22
Fluorescein-rhodamine B interface..... (27.3 in. well depth; 180 ml/min pumping rate)	23.5	37,500	81
Pumped water at end of 3d run..... (29.6 in. well depth; 180 ml/min pumping rate)	0.3	300	0
Pumped water at end of 4th run..... (33.8 in. well depth; 80 ml/min pumping rate)	1.0	1,460	2

neath the well coincided approximately at the 50% relative concentration level in a salinity-depth profile.

The relative concentration, ϵ , is defined as

$$\epsilon = c - c_b/c_s - c_b \quad (1)$$

where

c = measured salinity at point Z

c_b = background salinity of displaced water

c_s = salinity of sea water.

The relative salinity values at the upper boundary of the fluorescein zone and fluorescein-rhodamine B interface were computed from the measurements of salinities for each sample taken from those interfaces during the third run with a 0.69 m (27.3 in.) well penetration depth and a 180 ml/min pumping rate. The former and the latter were respectively 22 and 81%. With these two salinity values and those of fresh water and salt water, the location of the assumed sharp interface could be calculated using a theoretical concentration distribution as shown later in the dispersion section.

Only vertical one-dimensional upconing directly beneath a well was studied. The sea water-freshwater interface rose as the fresh water was pumped. The upconing height increased as pumping time elapsed until the interface reached an equilibrium condition. This upconing phenomenon was previously observed by Gee in a series of laboratory experiments.* Figure 9 shows the changes of upconing height in accordance with elapsed pumping time. In this figure, upconing at a 80 ml/min pumping rate was obtained from this study while the others were from Gee's previous study. The sharp interface upconing was computed based on 50% relative salinity in this study, while it was expressed by the fluorescein-rhodamine B interface in Gee's study.

Analysis of results of this study show that the elevation of the interface beneath the well increases as the well pumping rate or the well penetration depth is increased (Fig. 10). The dimensionless quantities of pumping rate, \hat{Q} ; upconing height, \hat{Z} ; and well penetration depth, \hat{d}_w , as used in Figure 10 are defined as

$$\hat{Q} = Q/H_e W K_z \quad (2)$$

$$\hat{Z} = Z/H_e \quad (3)$$

and

$$\hat{d}_w = d_w/H \quad (4)$$

where

Q = pumping rate

H_e = initial freshwater lens thickness

K_z = vertical hydraulic conductivity

W = thickness of sand-box model

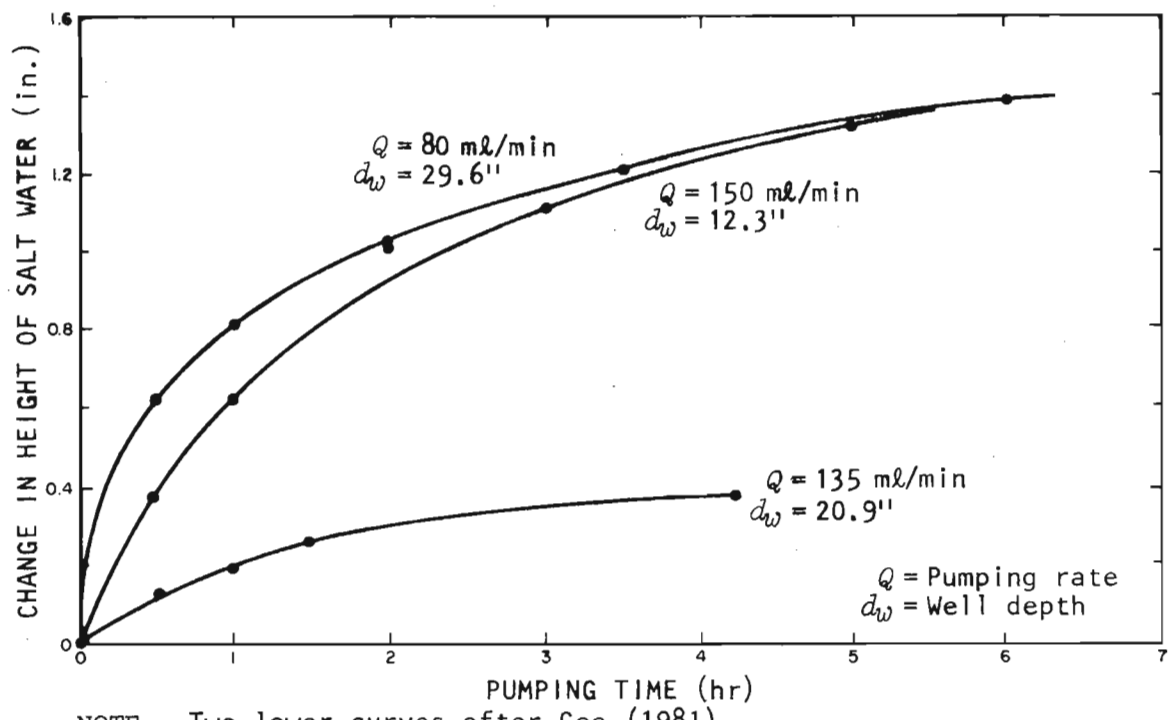
Z = elevation of upconed sharp interface
above initial sharp interface beneath well

d_w = well penetration depth from water table.

All the significant variables were included in defining dimensionless pumping rate.

A differently defined, dimensionless upconing height and partial well penetration depth was used. Figure 11 shows that the dimensionless upconing height, Z/d , increases as the dimensionless partial well penetration depth, d_w/d , and dimensionless pumping rate, \hat{Q} , increase; and d is the distance between the well bottom and initial sharp interface.

*H.K. Gee (1981): unpublished manuscript.



NOTE: Two lower curves after Gee (1981).

Figure 9. Upconing height vs. elapsed pumping time

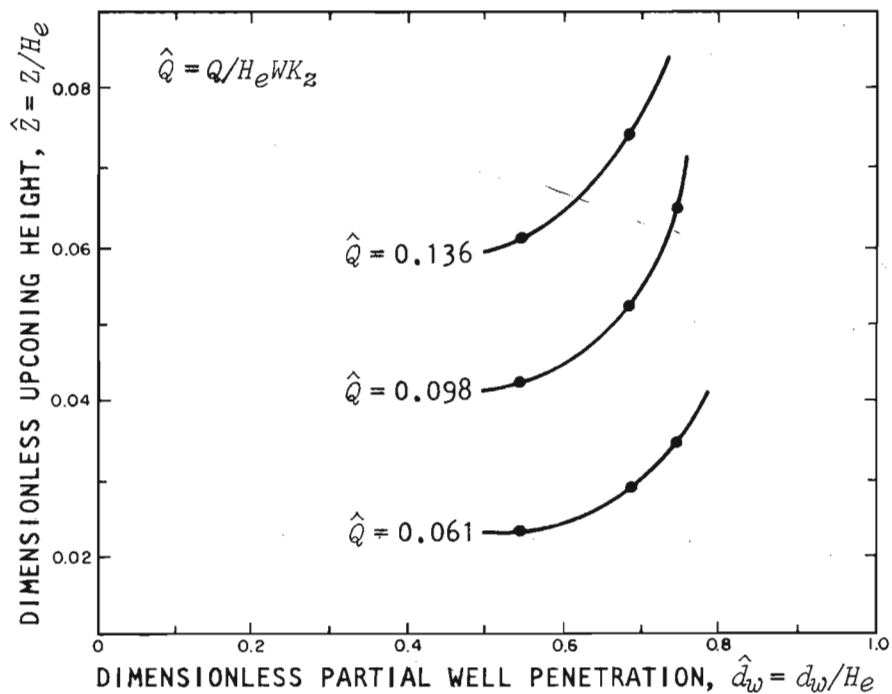


Figure 10. Effect of well penetration and pumping rate on upconing height

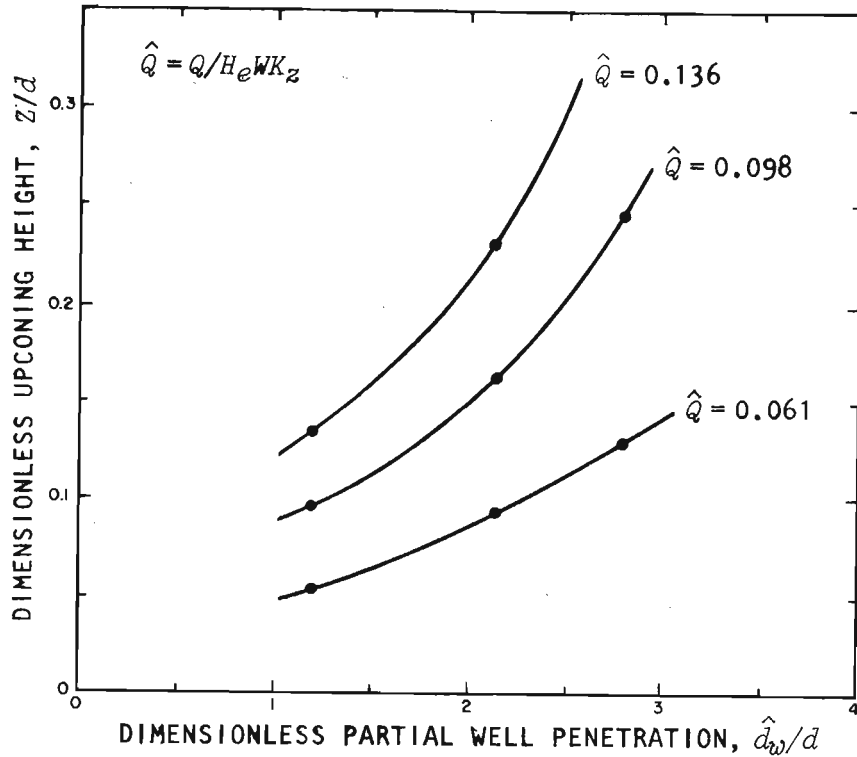


Figure 11. Dimensionless upconing height vs. dimensionless partial well penetration

The theoretical upconing height equation beneath the well at the equilibrium condition developed by Bear and Dagan (1964) is

$$Z(r = 0, t = \infty) = \frac{Q}{2\pi d (\Delta Y/Y) K_x} \quad (5)$$

where

Z = upconing height beneath well at equilibrium condition

Q = pumping rate

d = initial distance between bottom of well and center of interface

ΔY = density difference between sea water and fresh water

Y = density of fresh water

K_x = horizontal hydraulic conductivity of aquifer.

Equation (5) was derived for an infinite radial symmetric flow domain that is different from this experimental flow condition. In the sand-box model, there are some boundary effects on the sea water movement. However, these effects are probably minor. Further investigations are required before definitive discussions on this subject can be made.

To investigate the upconing in the sand-box model which had an approxi-

TABLE 2. UPCONING HEIGHT AND THICKNESS OF TRANSITION ZONE
DIRECTLY BENEATH WELL

RUN NO.	DIMENSIONLESS WELL PENETRATION DEPTH (EQ. 4)	DIMENSIONLESS PUMPING RATE (EQ. 2)	DIMENSIONLESS UPCONING HEIGHT (EQ. 3)		THICKNESS OF TRANSITION ZONE (in.)
			Measured	Computed	
1	0.54	0	0	0	0.30
		0.061	0.024	0.011	0.53
		0.099	0.043	0.017	0.71
2	0.68	0	0	0	0.37
		0.060	0.030	0.015	0.06
		0.098	0.052	0.024	0.75
		0.136	0.074	0.035	0.98
3	0.74	0	0	0	0.30
		0.061	0.034	0.018	0.75
		0.098	0.065	0.030	1.14
		0.136*	Up to well	-----	-----
4	0.84	0	0	0	0.90
		0.061*	Up to well	-	-----

*Excluded in analysis because of inclined interfaces (i.e., they were not one-dimensionless flow conditions).

mate horizontal one-dimensional freshwater flow condition, equation (5) was used. In a dimensionless form using dimensionless quantities defined previously in equations (2) and (3), equation (5) is rewritten as

$$\hat{Z}(r = 0, t = \infty) = \frac{\hat{Q}W K_z}{2\pi d (\Delta\gamma/\gamma) K_x}. \quad (6)$$

The aquifer was assumed isotropic and horizontal hydraulic conductivity, K_x , was assumed to be the same as vertical hydraulic conductivity, K_z . The computed dimensionless upconing height (eq. [6]) and the measured values converted into dimensionless terms (eq. [3]) are shown in Table 2. Equations (2), (3), and (4) were respectively used for the dimensionless pumping rate, upconing height, and well penetration depth in Table 2. The computed dimensionless upconing heights were 39 and 53% of the measured ones.

The discrepancies between the laboratory measurements and computations by equations of upconing height may be due to the following reasons:

1. Difference between K_x and K_z
2. Experimental errors
3. Assumptions used in the derivation of eq. 5

4. Partial well penetration effects
5. Differences in the geometry of the flow domain between those in the derivation of equation (5) and in this study.

Determination of Dispersivity of Laboratory Sand

Hydrodynamic dispersion is the sum of the mechanical dispersion and molecular diffusion in a porous medium. The evolution of a freshwater-sea water transition zone is a direct result of hydrodynamic dispersion.

A one-dimensional diffusion equation with a step-function input can be solved analytically (Bear 1979, p. 271). A step function input is described mathematically as

$$C(x, t) = \begin{cases} 0, & x < 0 \\ C_0, & x > 0 \end{cases} \quad (7)$$

where

$C(x, 0)$ = concentration of solute at distance x and time 0

x = distance from $x = 0$ axis.

In this case, the concentration of the solute at distance x and time t is

$$C(x, t) = \int_0^\infty \frac{C_0}{\sqrt{4\pi Dt}} \exp\left[\frac{-(x - \xi)^2}{4Dt}\right] d\xi \quad (8)$$

which can be transformed by setting $u = (x - \xi)/\sqrt{4Dt}$ to obtain

$$C(x, t) = \frac{C_0}{2} \left[1 + \operatorname{erf}\left(\frac{x}{\sqrt{4Dt}}\right) \right] \quad (9)$$

where erf means the "error function" which is defined as

$$\operatorname{erf} M = \frac{2}{\sqrt{\pi}} \int_0^M \exp(-u^2) du$$

For the relative concentrations, ε , divide both sides by C_0 to obtain

$$\varepsilon = \frac{C(x, t)}{C_0} = \frac{1}{2} \left[1 + \operatorname{erf}\left(\frac{x}{\sqrt{4Dt}}\right) \right] \quad (10)$$

where D is the dispersion coefficient with dimension of $(\text{length})^2/\text{time}$.

The relation between dispersion coefficient and dispersivity, D_m , (Bear 1972) is

$$D = D_m \bar{V} \quad (11)$$

where \bar{V} is average flow velocity and D_m is the length dimension. In the normal distribution, the variance is

$$\sigma^2 = 2Dt . \quad (12)$$

When equation (11) is substituted in (12),

$$\sigma^2 = 2Dt = 2D_m \bar{V}t = 2D_m x \quad (13)$$

and $4Dt$ is respectively replaced by $4D_m x$ and $2\sigma^2$ in equation (10), then

$$\varepsilon = \frac{1}{2} \left[1 + \operatorname{erf} \frac{x}{2\sqrt{D_m x}} \right] \quad (14)$$

and

$$\varepsilon = \frac{1}{2} \left[1 + \operatorname{erf} \frac{x}{\sqrt{2} \sigma} \right]. \quad (15)$$

Equations (14) and (15) are in the same forms as the equations in Schmorak and Mercado (1969) even though they used $(x - \bar{x})$ instead of x . This is because in equations (7) to (15) the x represents the distance from the initial step input to the point of interest, while in their equations $(x - \bar{x})$ represents the same distance with the superposition of convection and diffusion.

Schmorak and Mercado (1969) developed the following equation to compute the thickness of transition zone,

$$\sigma_1 = [\sigma_0^2 + 2D_m x]^{\frac{1}{2}}, \quad (16)$$

where

$2\sigma_1$ = thickness of the resultant transition zone after traveled x

$2\sigma_0$ = thickness of the undisturbed transition zone

D_m = dispersivity with length unit

x = traveled distance of assumed sharp interface.

The thickness of transition zone is 2σ where σ is the standard deviation of the concentration or salinity distribution and is defined by

$$\sigma = \frac{1}{2} [(x)_{\varepsilon=15.9\%} - (x)_{\varepsilon=84.1\%}]. \quad (17)$$

The assumed sharp interface height and the thickness of transition zone were computed using the sigmoidal concentration distribution of equation (15). The σ was computed from the relative salinity values of samples as introduced previously and the traveled distance x which was superpositioned with the convection and the diffusion. The increase in the thickness of the transition zone for each run (Table 2) paralleled the pumping rate and the well penetration depth.

Schmorak and Mercado (1969) rearranged equation (16) for dispersivity

by inserting $\bar{Z} = x$, the traveled distance of the assumed sharp interface, as

$$D = \frac{\sigma_2^2 - \sigma_0^2}{2\bar{Z}} . \quad (18)$$

Since transition zones existed at the initial equilibrium conditions, then σ_0 was not zero in the experiments. Using equation (18), the dispersivities for the different pumping rates and well penetration depths were computed from the σ and \bar{Z} values. Figure 12 shows the changes of dispersivity with regard to pumping rate and well penetration depth. The dispersivity apparently increased as the pumping rate and well penetration increased. The change of dispersivity was also observed by Schmorak and Mercado (1969) in their field experiments. The dispersivity ranged from 0.51 to 2.03 mm

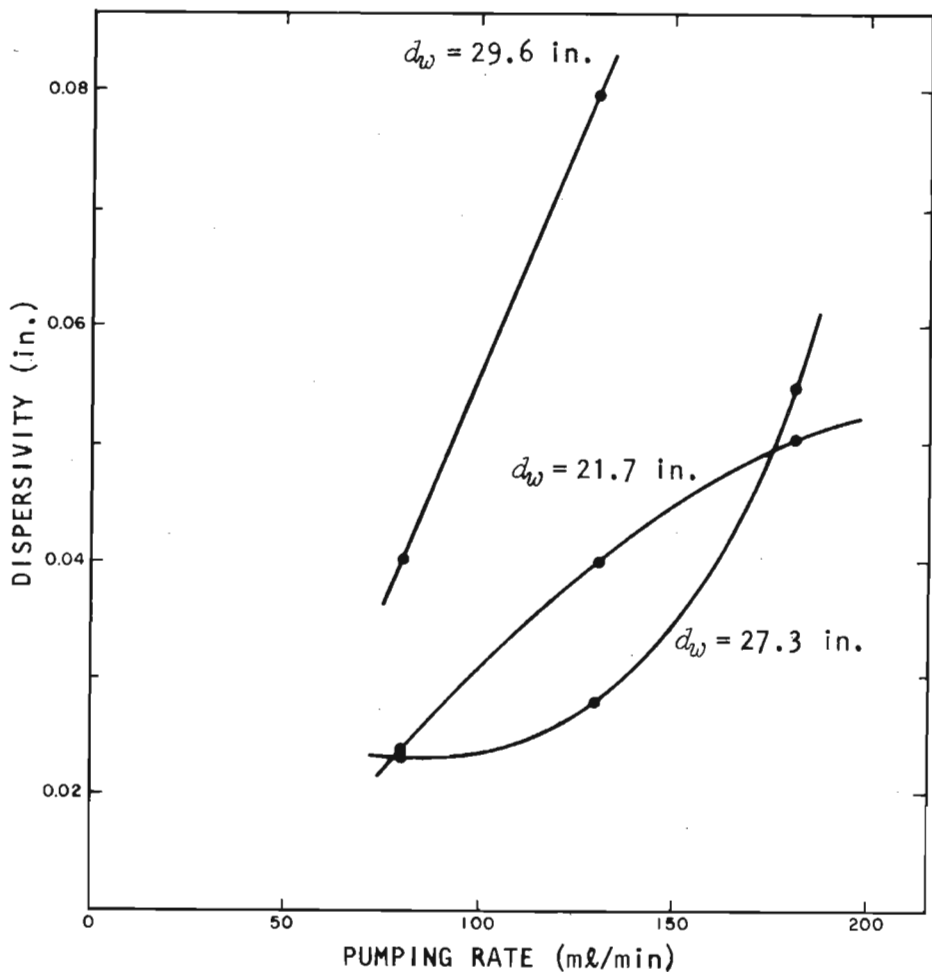


Figure 12. Dispersivity for different pumping rates

(0.02-0.08 in.) with an average of about 1.02 mm (0.04 in.) in this study, While this value is reasonable for the sand material used in the experiment, further investigations are needed to clarify the apparent variances in dispersivity.

Upconing with Transition Zone

Although an abrupt interface was assumed in the previous section, actually, a transition zone existed between the two miscible fluids because of hydrodynamic dispersion. The development of a transition zone can influence the relative concentration of salinity of pumped water; therefore, it should be considered in determining pumping rate and duration and well penetration.

Schmorak and Mercado (1969) introduced maximum permissible pumping rate equations which will ensure salt free water as

1. Assuming a sharp interface

$$Q_{\max} \leq 2\pi d (\Delta Y/Y) K_x Z_{\max} \quad (19)$$

2. Considering the transition zone

$$Q_{\max} \leq 2\pi d (\Delta Y/Y) K_x Z_{\max}^* \quad (20)$$

where

$Z_{\max} = \Theta d$ (maximum permissible upconing height assuming a sharp interface)

$Z_{\max}^* = \Theta d = (x - \bar{x})$ (maximum permissible upconing height considering the transition zone)

Θ = coefficient

$x - \bar{x}$ = distance from relative salinity of 50% to a predetermined relative salinity.

Equations (19) and (20) can be changed into dimensionless terms using (2) and (3) as

1. Assuming a sharp interface

$$\hat{Q}_{\max} \leq \frac{2\pi d (\Delta Y/Y) K}{W K_z} \hat{Z}_{\max} \quad (21)$$

2. Considering the transition zone

$$\hat{Q}_{\max} \leq \frac{2\pi d (\Delta Y/Y) K}{W K_z} \hat{Z}_{\max} \quad (22)$$

By using equation (21) with $\Theta = 0.5$, a \hat{Q}_{\max} value of 0.440 was obtained during the third run which is much larger than the applied dimensionless

pumping rate, 0.136. Equation (22), with 10% tolerable salinity, as determined previously showed a Q_{\max} value of 0.376. This is not surprising because the Θ value in Schmorak and Mercado's study was determined from field measurements of an Israeli sandstone aquifer whose porous medium differs considerably from the one used in this experiment. To use equations (21) and (22) for the experimental data in this study, the value of Θ should be from about 0.15 to 0.20.

CONCLUSIONS AND RECOMMENDATIONS

Based on this study the following conclusions and recommendations for succeeding studies can be made.

1. The sea water-freshwater interface rises as the pumping rate and/or well penetration depth increases
2. The transition zone between the sea water and fresh water thickens as the pumping time elapses at a given pumping rate
3. The theoretical equations derived previously by other investigators do not coincide with the experimental results; therefore, studies are needed to find out the reasons of these discrepancies
4. A larger model should be used so that (a) sampling will not influence nearby flow conditions and (b) the sampling of the intermediate points in the fluorescein zone can be possible
5. A continuously overflowing sea water reservoir should be used to maintain a precise sea water level
6. Chlorides should be used in lieu of salinity or electrical conductivity since the former will give more precise concentration measurements.

REFERENCES

American Society of Testing Materials. 1980. Permeability of granular soils. 1980 ASTM Manual, pt 19, D2434-68, pp. 362-67.

Bear, J. 1972. *Dynamics of fluids in porous media*. New York: American Elsevier.

_____. 1979. *Hydraulics of groundwater*. New York: McGraw-Hill.

_____, and Dagan, G. 1964. The unsteady interface below a coastal collector, Prog. Rep. 3, Hydraulic Laboratory, Israel Institute of Technology, Haifa, Israel.

- Chandler, R.L., and McWhorter, D.B. 1975. Upconing of the saltwater-freshwater interface beneath a pumping well. *Ground Water* 13(4): 354-59.
- Schmorak, S., and Mercado, A. 1969. Upconing of freshwater-seawater interface below pumping wells, field study. *Water Resour. Res.* 5(6):1290-1311.
- Todd, D.K. 1974. Upconing of saline water with particular reference to the Honolulu aquifer. In *Mathematical Modeling of Freshwater Aquifer Having Saltwater Bottoms*, GE TEMPO Report No. GE 74 TMP-43, pp. B1-B19.
- Vishner, F.N., and Mink, J.F. 1964. Ground-water resources in Southern Oahu, Hawaii. U.S. Geological Survey Water Supply Paper 1778.